**Technical Paper**

Journal of the Society of
Naval Architects of Korea
Vol. 25, No. 2, June 1988

# An Axially Marching Scheme for Internal Waves

by

Injoon Suh*

## Abstract

An axially marching numerical method is developed for the simulation of the internal waves produced by translation of a submersed vehicle in a density-stratified ocean. The method provides for the direct solution of the primitive variables $[v, p, \rho]$ for the nonlinear and steady state three-dimensional Euler's equation with a non-constant density term in the vehicle-fixed cartesian co-ordinate system.

By utilizing a known potential flow around the vehicle for an estimate of the axial velocity gradient, the present parabolic algorithm allows local upstreamwise disturbances and axial velocity variation.

## Nomenclature

$S_p(x, y, z)$ : Forcing function in the Poisson type equation for the pressure

$H$ : Vertical size of the computational domain

$B$ : Lateral size of the computational domain

$D$ : Maximum diameter of the vehicle

$L$ : Overall length of the vehicle

$N$ : The Brunt Väisäläs frequency defined by Eq. 2 for the linear profile of density

$F_r$ : The densimetric Froude number defined by Eq. 1 for the linear profile of density

$n, i, j$ : Integers to indicate the location of the each cells in $x, y$ and $z$ direction, respectively

$i_n, j_n$ : Number of cells in $y$ and $z$ direction

$C_h, C_v$ : Phase velocity of the internal waves in lateral and vertical direction, used to specify a radiation condition

$k$ : Current step of the iteration

$g$ : Gravitational acceleration

$\Delta x, \Delta y, \Delta z$ : Spatial mesh sizes in $x, y$, and $z$ direction, respectively

$\Delta t$ : $=\Delta x$ in nondimensional term

$*$ : Nondimensional term

$F(x, y, z)$ : Vertical position marker

$\eta(x, y, z)$ : $=F(x, y, z)-F_0(z)$, Eulerian field of vertical displacement of the water particles

$(u_{po}, v_{po}, w_{po})$ : Velocity components obtained from potential flow calculation

$(x, y, z)$ : Vehicle-fixed co-ordinate system defined in Fig. 1

$(t, y, z)$ : Sensor-fixed co-ordinate system

$(u, v, w)$ : Instantaneous velocity components in $x, y$, and $z$ direction, respectively

$\rho$ : Instantaneous fluid density

$\rho_m$ : Undisturbed fluid density at the origin of the co-ordinate system

$p$ : Instantaneous pressure

$f_0$ : Undisturbded upstream magnitude of

Manuscript received: July 2, 1987, revised manuscript received: Feb. 27, 1988

* Member, Chin-hae research laboratory

the variable $f$, $f=u, v, w, p$ and $\rho$

$\hat{f}$ : Perturbations of the variable $f$, $f=u, v, w, p$ and $\rho$

$(x_p, y_p, z_p)$ : Position of the wave probe

$(\hat{x}, \hat{y}, \hat{z})$ : Displacement of a fluid particle initially positioned at $(x_p, y_p, z_p)$

$\Omega(x, y, z)$ : $=\frac{\partial v}{\partial y}+\frac{\partial w}{\partial z}$, Divergence of two dimensional velocity vector $(v, w)$ (Crossstream divergence), or axial velocity gradient

$\Omega_{po}(x, y, z)$ : Magnitude of $\Omega(y, z)$ obtained from potential flow calculation

## Introduction

The objective is to simulate three-dimensional internal waves generated by a steadily translating submerged vehicle through a density-stratified fluid in which the undisturbed upstream density is a continuous function of depth only.

In order to minimize computer storage requirements we needed to develop a numerical scheme which will, in effect, reduce the full three-dimensional (in space) steady state problem to a two-dimensional unsteady problem. This is accomplished by conceptually thinking of the $x$-axis as being replaced by the time axis. Thus the first step is to choose an axially marching scheme requiring that the induced flow is fully developed to a steady state.

Wessel[1] and Young and Hirt[2] formulated a time-dependent two-dimensional Euler's equation for internal wave development due to an initial wake-collapse by using a strong conservative system of primitive variables as in the "MAC" method originated by Harlow and Welch[3] and further improved by Nicols and Hirt[4], Chan and Street[5], Miyata and Nishimura[6], etc. This series of methods had several desirable features;

1) strong conservative character

2) being stable in the incompressible inviscid fluid

3) easy satisfaction of the free surface boundary condition and

4) an explicit algorithm for the velocity. These features are shared by the present algorithm

Although a steady three-dimensional flow and a unsteady two-dimensional one have several mathematical features in common, we have a difficulty in developing a marching procedure; the axial momentum equation and the cross-stream momemtum equations must be uncoupled in a marching configuration and consequently the three-dimensional continuity is difficult to satisfy, in general. That's why the axially marching scheme has been used for the special case where the axial velocity perturbation is small.

Since neglecting the axial velocity perturbation in a marching procedure gives an identical model to a time dependent two-dimensional problem(in an inviscid fluid), previous numerical studies on the internal wave mechanism used this approximation with different algorithms; Lewellen et al.[7] and Piacsek and Roberts[8] solved steady state three-dimensional internal waves by an axially marching scheme with assumption of no axial velocity perturbation.

This paper handles the axial velocity by a special treatment of the continuity equation, i.e., considering the axial velocity gradient, $\Omega(y, z)$, as a source, a pressure field in a cross-stream section is determined implicitly such that the corresponding velocity field in a cross-stream section satisfies the mass conservation with the existence of sources, $\Omega$.

The point is that $\Omega$ is assumed to be known from potential theory. Questions may be raised about this matching of the potential theory to the present inhomogeneous fluid problem, since the potential flow has no density effect. The explanation is that the buoyancy effect due to the density perturbation only acts on the cross-stream velocities, not on the axial velocity.

The only influences of the density perturbation on the axial velocity would be an indirect component resulting from satisfying the continuity equation.

Therefore an axial velocity gradient, $\Omega_{po}$, obtained from the potential theory can be a reasonable estimate of the real $\Omega$. In the far field aft the vehicle, the potential flow converges to the undisturbed flow hence the axial velocity gradient vanishes and also the continuity equation becomes two-dimensional.

This implies that the present algorithm is based on

the fact that, regardless of a substantial change of the axial velocity near the body, the vehicle-induced internal wave field itself has negligible axial component compared to cross-stream velocities. This fact has been proved by analytical investigators by obtaining small envelop angles in the wave pattern aft the body[10, 11, 12].

## Mathematical Formulation

An useful parameter for characterizing the present problem is the densimetric Froude number, $F_r$. We define this non-dimensional number as

$$F_r=\frac{2\pi u_0}{ND} \tag{1}$$

Where $u_0$ is the speed of the vehicle, $D$ its maximum diameter and $N$ is the Brunt Väisäläs frequency defined by

$$N^2=-\frac{g}{\rho_m}\frac{\partial \rho_0}{\partial z} \tag{2}$$

For the case of two uniform layers seperated by a thin transition layer, the maximum value of $N$ would be used to define the densimetric Froude number.

To handle the axial velocity near the body, which affects the far field wave, the axial velocity gradient $\Omega$ in the potential flow has to be monitored in the whole domain until the potential disturbance due to the body displacement has decresed to a negligible amount.

The matching is reasonable provided that the near field potential flow dominates in the near domain and the perturbed flow due to the cumulative effect of the perturbed density term dominates in the far domain. Euler's system of equations may be a good model for the simulation of the far field internal wave flow due to the presence of non-uniform density. But, the solution of this primitive variable system requires a lot of special effort to treat the irregular body boundaries. Thus a simple way to get rid of this difficulty was a "slender body approximation". It is, however, easily seen that the full continuity equation near the body was not satisfied. Since this simple boundary treatment may cause a serious overestimation of far field internal waves, the accurate model for the vehicle in the near domain is crucial for good estimates of the far-field wave. Therefore, the present method of matching procedure is designed to specify an exact vehicle boundary condition especially for a non-slender body.

To reduce the dimensionality of the problem, restrict attention to steady (in time) disturbances relative to a co-ordinate system fixed in the vehicle, i.e., "trapped" internal wave modes with phase velocities equal to the forward speed of the vehicle. The vehicle is considered to be fixed within a control volume and encounters an imposed flow with an upstream undisturbed velocity, $u_0$, equal to the prescribed forward speed of the vehicle.

A right-handed cartesian co-ordinate system is used with the origin fixed in the center of the near domain, (see Fig. 1) the $x$-axis lies along the longitudinal axis of the control volume and is positive in the down stream direction, the $z$-axis is along the vertical and oppositely directed to gravity, and the $y$-axis is directed laterally across the stream to produce a righthanded co-ordinate system.

Keeping the nonlinear inertial terms in steady state three-dimensional Euler's equation, the independent variables $(x, y, z)$ are to be transformed to $(u_0t, y, z)$, i.e., transform the body-fixed frame into the tank-fixed system of reference(or sensor-fixed reference) to lead to a time dependent two-dimensional system of equations.

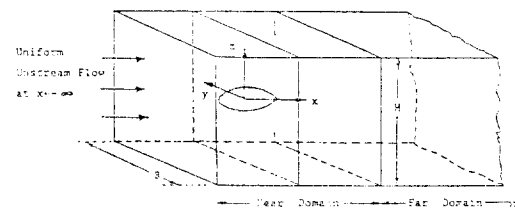


**Fig. 1** Co-ordinate system for vehicle placed in the fluid domain

The system of equations are reduced to

$$\frac{\partial v}{\partial t}+\frac{\partial v^2}{\partial y}+\frac{\partial wv}{\partial z}=-\frac{\partial \hat{p}}{\partial y}+\frac{\nu}{Du_0}\left(\frac{\partial^2}{\partial t^2}+\Gamma^2\right)v$$

$$\frac{\partial w}{\partial t}+\frac{\partial vw}{\partial y}+\frac{\partial w^2}{\partial z}=-\frac{\partial \hat{p}}{\partial z}+\frac{\nu}{Du_0}\left(\frac{\partial^2}{\partial t^2}+\Gamma^2\right)w-\frac{gD}{u_0^2}(\rho-\rho_0)$$

$$(1+\hat{u}_{po})\frac{\partial \rho}{\partial t}+v\frac{\partial \rho}{\partial y}+w\frac{\partial \rho}{\partial z}=0$$

$$\frac{\partial v}{\partial y}+\frac{\partial w}{\partial z}=\Omega_{po}(t,y,z) \tag{3}$$

where $\hat{u}_{po}$ and $\Omega_{po}$ are obtained from the potential theory and from the relation

$$\Omega_{po}=\frac{\partial v_{po}}{\partial y}+\frac{\partial w_{po}}{\partial z}=-\frac{\partial \hat{u}_{po}}{\partial t} \tag{4}$$

where $v_{po}$, $w_{po}$ and $\hat{u}_{po}$ are the disturbed velocity components due to the presence of the body obtained from source distribution method.

The displacement of a fluid particle at time $t$ from its undisturbed position can be calculated by particle tracing. However, the present objective is the simulation of wave probe measurements which are different from the Lagrangian particle trace. (Of course both were very close throughout the research.) The kinematic condition for the deformation of the horizontal planes of constant density is

$$\frac{DF}{Dt}=0 \tag{5}$$

where 'F' denotes the vertical position marker which, in turn, becomes

$$(1+\hat{u}_{po})\frac{\partial F}{\partial t}+v\frac{\partial F}{\partial y}+w\frac{\partial F}{\partial z}=0 \tag{6}$$

and whose initial condition at the undisturbed upstream is

$$F_0(z)=z \tag{7}$$

As a limiting case, if the initial density stratification is linear given by the relation

$$\rho_0(z)=-N^2\rho_m z/g \tag{8}$$

in dimensional terms or

$$\rho_0(z)=-N^2 D z/g \tag{9}$$

in nondimensional term, where $\rho_0$ actually means $\rho_0-\rho_m$. Then by comparing Eq. 7 and 9, the relation

$$F=-\rho g/(N^2 D) \tag{10}$$

is obtained. Thus for this limiting case, by calculating the Eulerian density field the Eulerian field of the vertical displacement of the particle, $\eta(y,z)$, is obtained by the above Eq. 10, and the relation

$$\eta(t,y,z)=F(t,y,z)-F_0(z) \tag{11}$$

The far upstream boundary condition (initial condition), $\hat{u}_0, v_0, w_0$ and $\hat{p}_0$, are chosen to be zero if the initial $x$ is chosen to be a negative infinity.

The sommerfeld radiation condition

$$\frac{\partial f}{\partial t}\pm C_h\frac{\partial f}{\partial y}=0 \tag{12}$$

was used for the artificial boundaries of the rectangular computational domain. '$C_h$' denotes the phase velocity in the horizontal direction and '$f$' is used to denote $v, w$ and $\rho$. '+' is used for the boundary of positive $y$ and '−' is for the boundary of negative $y$.

Similarly, for the upper and lower boundaries,

$$\frac{\partial f}{\partial t}\pm C_v\frac{\partial f}{\partial z}=0 \tag{13}$$

where $C_v$ denotes the phase velocity in the vertical direction. $C_h$ and $C_v$ are chosen to be constants assuming the normal component of internal wave celerity at each boundary is not a function of $y$ or $z$. For the estimate of $C_h$ and $C_v$, numerical results of the simplified model for the restricted channel boundary are utilized.

By adding the differentiation of the $y$-momentum equation (Eq. 3) with respect to $y$ to the differentiation of the $z$-momentum equation (Eq. 3) with respect to $z$, the Poisson type equation for pressure

$$\nabla^2\hat{p}=-\frac{\partial}{\partial t}(\Omega)-2\frac{\partial^2 vw}{\partial y\partial z}-\frac{\partial^2 v^2}{\partial y^2}-\frac{\partial^2 w^2}{\partial z^2}+\frac{\nu}{Du_0}\left(\frac{\partial^2}{\partial t_2}+\nabla^2\right)(\Omega)-\frac{gD}{u_0^2}\left(\frac{\partial \rho}{\partial z}-\frac{\partial \rho_0}{\rho z}\right) \tag{14}$$

is obtained. This is the governing equation for the pressure which is to be solved iteratively with the Neumann type boundary condition defined in Eq. 3

## Numerical Algorithm

The main procedure of the method is to obtain the $(y,z)$ distribution of the dependent variables at time step $n$ and then use this information to move to the time step $n+1$. The fundamental assumption in thinking of the $x$-axis as being replaced by a time axis, is that perturbations propagate only forward in time and downstream, i.e., the results obtained at $x=x^n$ do not change the values at $x=x^{n-1}$ but do affect the values at $x=x^{n+1}$. For convenience we call this basic scheme an "axially marching" method.

This procedure is particularly appropriate to our application since the steady internal wave field has

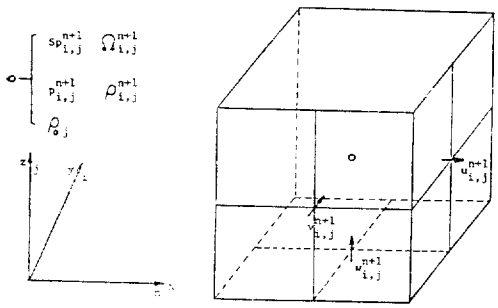

**Fig. 2** 3-Dimensionally staggered grid system

negligible up-streamward disturbances due to a dominant axial-advection in the system of equation, except near the body.

In order to consider an axial velocity perturbation, which is not negligible near the vehicle, the slenderness assumption, $\Omega=0$, is removed in this paper.

Every grid in $y-z$ plane can act as a numerical source cell which has non-zero divergence, $\Omega_{po}$. This new concept is possible since the known potential flow determines the strengths of each numerical source cells in the $y-z$ plane at every step in time. This arrangement, actually handles the effect of the axial velocity component.

$\hat{u}^{n+1}_{i,j}$ at the position shown in Fig. 2 has to be obtained by the potential theory to calculate $-\frac{\partial \hat{u}_{po}}{\partial t}$ which, in turn, determines $\Omega_{po}$.

This $\Omega_{po}$ is used to dertermine the forcing function of the pressure, $S_p$, as if $\Omega_{po}$ is the strength of the sources distributed over the $y-z$ plane. For the fine meshes, the relation,

$$\Omega_{po}(t, y, z)=-\frac{\partial \hat{u}_{po}}{\partial t} \tag{15}$$

was reasonable but for the coarse meshes the direct calculation

$$\Omega_{po}(t, y, z)=\frac{\partial v_{po}}{\partial y}+\frac{\partial w_{po}}{\partial z} \tag{16}$$

is an alternative method, where the subscript '*po*' denotes the potential flow. The latter was proved to be more favorable for the large cells and for the very displaced body case.

The computational fluid domain is divided by three types of cells: fluid cell, boundary cell and vehicle cell which are flagged by letters $F, B$ and $V$, respectively.

The 3-dimensional fluid domain is divided into two regions, i.e., a near domain and a farfield domain as shown in Fig. 1. The axial grid size $\Delta x$ (or $\Delta t$), in cases, has different values between near and far domain; Since the stability of the scheme depends on the stream speed, $\Delta x$ for the whole domain must be chosen to depend on the speed. Additionally, $\Delta x$ in the near domain must be chosen to be small enough to obtain a good resolution of the vehicle geometry. Thus $\Delta x$ in the near domain is less or equal to $\Delta x$ in the far domain with no exception.

The present semi-implicit computation has stability criteria.

$$\Delta t/\Delta y<0.5 \tag{17}$$

and the C.F.L.(Courant, Friedrichs and Lewy) condition for the present internal wave problem depends on the densimetric Froude nember i.e.,

$$\Delta t/\Delta y<F_r/32 \tag{18}$$

## Pressure Solution

The Poisson type of the pressure equation (Eq. 14) is approximated by the 2-nd order central difference in space.

$$(\hat{p}^{n+1}_{i+1,j}-2\hat{p}^{n+1}_{i,j}+\hat{p}^{n+1}_{i-1,j})/\Delta y^2$$
$$+(\hat{p}^{n+2}_{i,j+1}-2\hat{p}^{n+1}_{i,j}+\hat{p}^{n+1}_{i,j-1})/\Delta z^2=Sp^n_{i,j} \tag{19}$$

where the superscript '$n+1$' denotes the new step of time and the subscript $i$ and $j$ denote the position in $y$ and $z$ direction respectively.

The forcing function $Sp^n_{i,j}$ is approximated by the 2-nd order central difference in space and first order forward difference in time.

$$Sp^n_{i,j}=-(\Omega^{n+1}_{poi,j}-\Omega^n_{i,j})/\Delta t$$
$$-[(v^n_{i+1,j}+v^n_{i+1,j+1})(w^n_{i-1,j+1}-w^n_{i,j+1})$$
$$+(v^n_{i,j}+v^n_{i,j-1})(w^n_{i,j}+w^n_{i-1,j})$$
$$-(v^n_{i+1,j}+v^n_{i+1,j-1})(w^n_{i+1,j}+w^n_{i,j})$$
$$-(v^n_{i,j+1}+v^n_{i,j})(w^n_{i,j+1}+w^n_{i-1,j+1})]/2\Delta y\Delta z$$
$$-[(v^n_{i+2,j}+v^n_{i+1,j})^2-2(v^n_{i+1,j}+v^n_{i,j})^2$$

a) $u_o$ = 5.493 Cm/s, Fr = 11.20

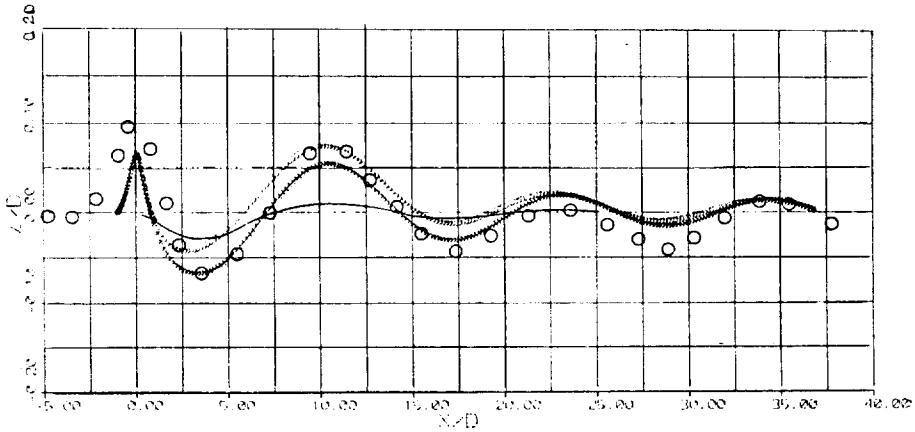


b) $u_o$ = 3.081 Cm/s, Fr = 6.28

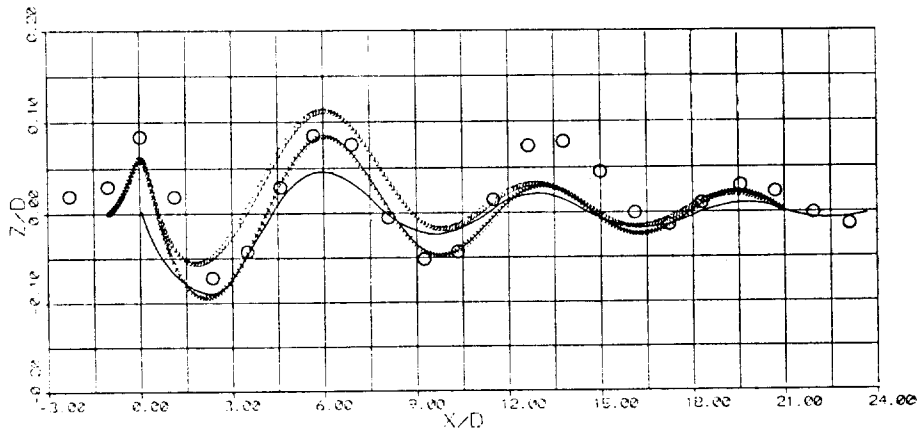


c) $u_o$ = 2.483 Cm/s, Fr = 5.06

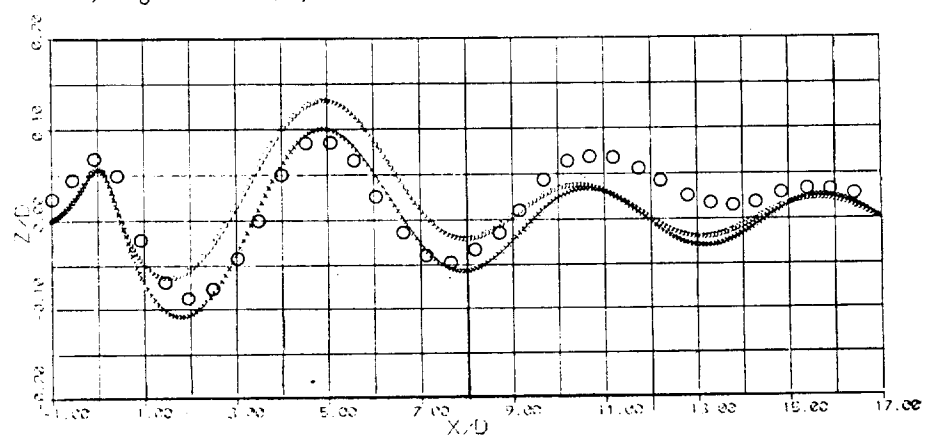

d) $u_0$ = 2.040 Cm/s, Fr = 4.16

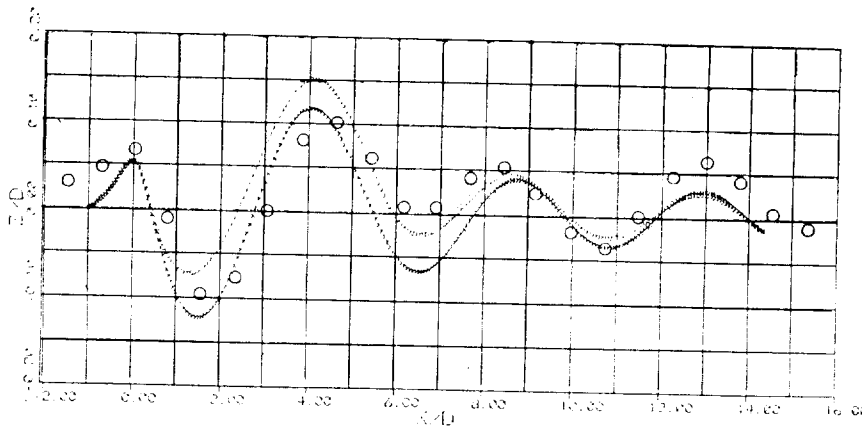

e) $u_0$ = 1.540 Cm/s, Fr = 3.14

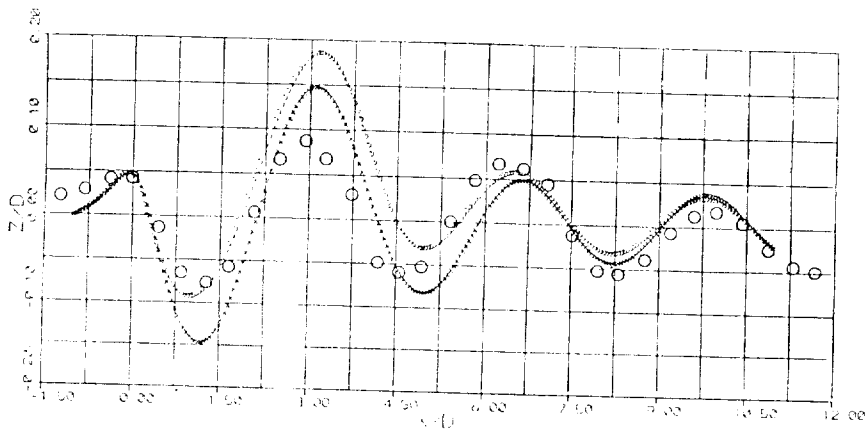

f) $u_0$ = 1.025 Cm/s, Fr = 2. 09

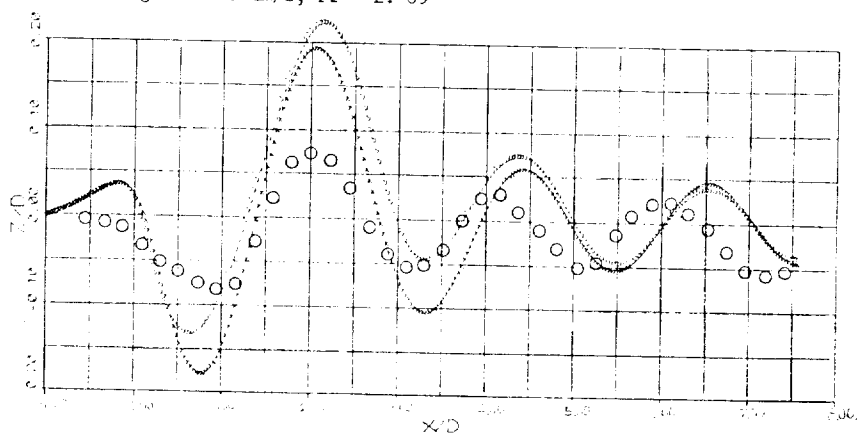

o o o o : Present nonlinear calculation
× × × × : Linear approximation
○ : Experiment by lofquist
—— : Analytical result by lofquist

**Fig.** 3 Particle displacement sampled at $Zp/D$=1.0 $Yp/D$=0 for a sphere in the linear stratification ($D$=4.761cm, $N$=0.647rad/s)

$$+(v^n_{i,j}+v^n_{i-1,j})^2]/\Delta y^2$$

$$-[(w^n_{i,j+2}+w^n_{i,j+1})^2-2(w^n_{i,j+1}+w^n_{i,j})^2$$

$$+(w^n_{i,j}+w^n_{i,j-1})^2]/\Delta z^2$$

$$+\frac{\nu}{Du_0}[(\Omega^n_{i+1,j}-2\Omega^n_{i,j}+\Omega^n_{i-1,j})/\Delta y^2$$

$$+(\Omega^n_{i,j+1}-2\Omega^n_{i,j}+\Omega^n_{i,j-1})/\Delta z^2]$$

$$-\frac{gD}{u_0{}^2}[(\rho^n_{i,j+1}-\rho^n_{i,j-1})/2\Delta z-$$

$$(f_{0j+1}-f_{0j-1})/2\Delta z] \quad (20)$$

All the terms in $Sp^n_{i,j}$ are determined in the previous time step $n$ except the term $\Omega^{n+1}_{poi,j}$ which is derived from the potential theory.

$$\Omega^{n+1}_{poi,j}=(v^{n+1}_{poi+1,j}-v^{n+1}_{poi,j})/\Delta y+(w^{n+1}_{poi,j+1}-w^{n+1}_{poi,j})/\Delta z \quad (21)$$

where the midscript '$po$' implies the values from the potential theory.

And $\Omega^n_{i,j}$ at the previous time step is obtained by

$$\Omega^n_{i,j}=(v^n_{i+1,j}-v^n_{i,j})/\Delta y+(w^n_{i,j+1}-w^n_{i,j})/\Delta z \quad (22)$$

The iterative expression of the finite differenced Poisson equation is

$$\hat{p}^{k+1}_{i,j}=a_1\hat{p}^k_{i+1,j}+a_2\hat{p}^k_{i-1,j}+a_3\hat{p}^k_{i,j+1}$$

$$+a_4\hat{p}^k_{i,j-1}+a_5Sp_{i,j} \quad (23)$$

where

$$a_1=a_2=\Delta z^2/(2\Delta y^2+2\Delta z^2)$$

$$a_3=a_4=\Delta y^2/(2\Delta y^2+2\Delta z^2)$$

$$a_5=-\Delta y^2\Delta z^2/(2\Delta y^2+2\Delta z^2)$$

where the superscript '$k$' and '$k+1$' denote the iteration step understanding that the desired time step is fixed at $n+1$.

This iteration is applied at the "fluid" and "vehicle" cells. Since the coefficients $a_1$ through $a_4$ are less than unity this iteration is unconditionally convergent.

For the boundary cells, the above derived relations can not be applied due to the finite grid. For this reason, the simple one sided difference

$$\hat{p}^{k+1}_{1,j}=\hat{p}^{k+1}_{2,j}-\frac{\partial\hat{p}}{\partial n}\Delta y \quad (24)$$

is used by utilizing the prepared information of the Neuman type boundary condition $d\hat{p}/dn$ which had been obtained in the Eq. 25 and 26, by substituting the proper values of $i, j$ and $n$. Regardless of the type of boundaries, the Neumann type of the pressure boundary condition is required.

## Velocity Solution

The conservative form of the equation 3 are approximated by the forward difference in time and the central difference in space $y$ and $z$.

$$(v^{n+1}_{i,j}-v^n_{i,j})/\Delta t+[(v^n_{i,j}+v^n_{i+1,j})^2$$

$$-(v^n_{i-1,j}+v^n_{i,j})^2]/4\Delta y$$

$$+[(v^n_{i,j+1}+v^n_{i,j})(w^n_{i,j+1}+w^n_{i-1,j+1})$$

$$-(v^n_{i,j}+v^n_{i,j-1})(w^n_{i,j}+w^n_{i-1,j})]$$

$$/4\Delta z=-(\hat{p}^{n+1}_{i,j}-\hat{p}^{n+1}_{i-1,j})/\Delta y$$

$$+\frac{\nu}{Du_0}[(v^n_{i+1,j}-2v^n_{i,j}+v^n_{i-1,j})/\Delta y^2$$

$$+(v^n_{i,j+1}-2v^n_{i,j}+v^n_{i,j-1})/\Delta z^2] \quad (25)$$

$$(w^{n+1}_{i,j}-w^n_{i,j})/\Delta t+[(v^n_{i+1,j}+v^n_{i+1,j-1})(w^n_{i+1,j}+w^n_{i,j})$$

$$-(v^n_{i,j}+v^n_{i,j-1})(w^n_{i,j}+w^n_{i-1,j})]/4\Delta y$$

$$+[(w^n_{i,j+1}+w^n_{i,j})^2-(w^n_{i,j}+w^n_{i,j-1})^2]/4\Delta z$$

$$=-(\hat{p}^{n+1}_{i,j}-\hat{p}^{n+1}_{i,j-1})/\Delta z+\frac{\nu}{Du_0}[(w^n_{i-1,j}-2w^n_{i,j}$$

$$+w^n_{i-1,j})/\Delta y^2+(w^n_{i,j+1}-2w^n_{i,j}+w^n_{i,j-1})/\Delta z^2]$$

$$-\frac{gD}{u_0{}^2}[(\rho^n_{i,j}+\rho^n_{i,j-1})/2-(f_{0j}+f_{0j-1})/2] \quad (26)$$

The perturbed density equation is approximated

$$(1+\tilde{u}^n_{poi,j})(\rho^{n+1}_{i,j}-\rho^n_{i,j})/\Delta t+(v^n_{i,j}+v^n_{i-1,j})$$

$$(\rho^n_{i+1,j}-\rho^n_{i-1,j})/4\Delta y+(w^n_{i,j}+w^n_{i,j+1})$$

$$(\rho^n_{i,j+1}-\rho^n_{i,j-1})/4\Delta z=0 \quad (27)$$

For "boundary" cells, the Sommerfeld radiation condition is approximated by the forward difference in time and space to obtain

$$f^{n+1}_{in,j}=-C_k\frac{\Delta t}{\Delta y}(f^n_{in,j}-f^n_{in-1,j})+f^n_{in,j} \quad (28)$$

for the positive $y$ boundary with $j=2, 3, \cdots, jn$

$$f^{n+1}_{1,j}=-C_k\frac{\Delta t}{\Delta y}(f^n_{1,j}-f^n_{2,j})+f^n_{1,j} \quad (29)$$

for the negative $y$ boundary with $j=2, 3, \cdots, jn$

$$f^{n-1}_{i,jn}=-C_v\frac{\Delta t}{\Delta z}(f^n_{i,jn}-f^n_{i,jn-1})+f^n_{i,jn} \quad (30)$$

for the positive $z$ boundary with $i=1, 2, \cdots, in$ and

$$f^{n-1}_{i,1}=-C_v\frac{\Delta t}{\Delta z}(f^n_{i,1}-f^n_{i,2})+f^n_{i,1} \quad (31)$$

for the negative $z$ boundary with $i=1, 2, \cdots, in$

where $C_h$ is the horizontal phase velocity, $C_v$ is the vertical phase velocity and $f$ denotes the variable $v$, $w$ and $\rho$.

## Numerical Calculations

The numerical simulations, based on the present algorithm were conducted for the linear stratification. A known potential flow around a sphere was chosen for an illustration of the method.

Since the known experimental studies were for the case of the linear stratification, a series of the numerical simulations were designed to meet the specific test conditions of the available experimental data for the verification of the present method.

For the numerical calculations for a sphere of diameter 4.761cm running through the linearly stratified fluid of N=0.647 radian per second, the aspect ratio of the Rankine ovoid was chosen to be 1. Six different Froude number cases were made for speeds of 5.493 through 1.025cm/sec which were selected to correspond to those in the experiment by Lofquist [9].

Fig. 3 presents the particle displacements sampled at $Zp/D=1.0$ and $Yp/D=0$ for 6 different vehicle speeds. In each figure, the present numerical calcu-

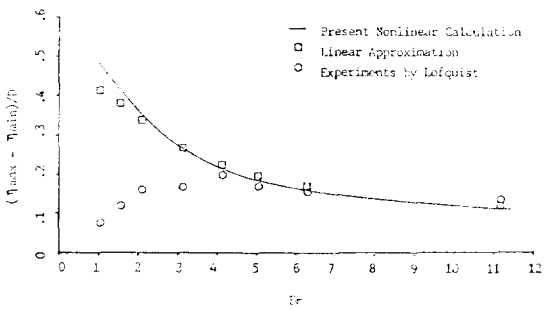


**Fig. 4** Fr. vs. maximum wave height sampled at $Zp/D=1.0$ $Yp/D=0$ for a sphere in the linear stratification

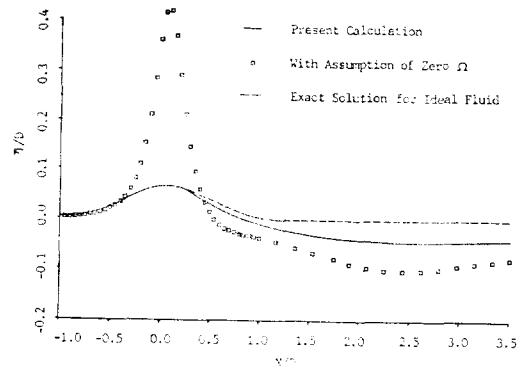


**Fig. 5** Particle displacement sampled at $Zp/D=1.0$ $Yp/D=0$ for a sphere in the linear stratification: comparison of two different methods ($D=4.761$cm, $N=0.647$rad/s, $uo=5.493$cm/s, $Fr=11.2$)

lation was compared with the Lofquist's experimental result and with the Lofquist's analytical solution. For each run, the numerical calculation was carried out for both nonlinear and linear system of equations.

Throughout the present study, the results of the linear system were in a reasonable agreement with the nonlinear results. It is noted that the linear system was obtained by setting the cross-stream adv ection terms be zero in the governing equations (Eq. 3). The main feature of the nonlinearity observed in these figures was the asymmetry of the upper and lower half amplitudes due to the cross-stream advection.

In terms of the wave lengths, the numerical results were nearly identical to the experimental results. For Fr>3, the numerical results of the wave amplitude agreed with the experiments reasonably, but for the extremely slow speed cases shown in Fig. 4 the numerical results disagreed with the experiments. Comparison of the present method with the slender body approximation (assumption of zero $\Omega$) is shown in Fig. 5. The slender body theory overestimates about 6 times the present result for the sphere.

## Conclusions

It appears that the present matching technique in an axially marching scheme would have been a new

and useful tool to have estimate of the magnitude of the vehicle-induced phenomena in the stratified fluid.

Since the present numerical simulation results were reasonably consistent with the experimental results, there is an enhanced confidence in prototype predictions obtained with the numerical experiments.

The axial velocity in the marching procedure, which has been proved to be very crucial factor for this kind of problems, could be handled due to a special treatment of the continuity equation: in the primitive variable system (i.e., pressure-divergence system $[P, \Omega]$), the pressure is calculated iteratively such that the corresponding velocity field satisfies the full continuity equation, by using a unique form of the kinematic boundary condition of the vehicle, i.e., the axial velocity gradient (or cross-plane divergence), $\Omega_{po}(x, y, z)$, which is evaluated from the potential theory.

Consequent features of the present algorithm are:

1) The present axially marching algorithm substantially reduces the computer-storage requirement for a three-dimensional fluid domain.

2) The vehicle-boundary condition is easy to specify. The matching procedure eliminates the difficulty of imposing complex boundaries in the rectangular grid system. Furthermore, faster convergence in the iteration is obtained in the matching procedure than in the local boundary treatment as in the slender body approximation. The reason is that the boundary condition, $\Omega_{po}(x, y, z)$, is distributed continuously over a cross-section while the usual boundary condition has a discontinuity.

3) The downstream boundary condition is not necessary for this axially marching scheme.

4) The disadvantage would be that the potential flow in the homogeneous fluid due to the rigid displacement must be known for the estimate of the axial velocity.

## References

[1] Wessel, W.R., "Numerical Study of the Collapse of a perturbation in an Infinite Density Stratified Fluid", The Physics of Fluids, Supplement II, 1969.

[2] Young, J.A. and Hirt, C.W. "Numerical Calculation, of Internal Wave Motions", *J. Fluid. Mech.* 56, p. 265, 1972.

[3] Harlow, F.H. and Welch, J.E., "Numerical Calculation of Time-Dependent Viscous Incompressible Flow of Fluid with Free Surface", The Physics of Fluids, vol. 8, No. 12, Dec. 1965.

[4] Nichols, B.D. and Hirt, C.W., "Improved Free Surface Boundary Conditions for Numerical Incompressible-Flow Calculations," *J. Comp. Physics* 8, 434-448, 1971.

[5] Chan, R.K.C. and Street, R.L., "A computer study of Finite-Amplitude Water Waves," *J. Comp. Physics* 6, 68-94, 1970.

[6] Miyata, H. and Nishimura, S., "Finite-difference simulation of nonlinear ship waves", *J. Fluid. Mech.* 157, 327-357, 1985.

[7] Lewellen, M.S. et al. "Turbulent Wakes in a Stratified Fluid, Part 1: Model Development, Verification, and Sensitivity to Initial Conditions", A.R.A.P. Report No. 226, Aeronautical Research Associates of Princeton, Inc. Aug. 1974.

[8] Piacsek, S.A. and Roberts, G.O. "Numerical Experiments on Collapsing Wakes in a Stratified Ocean", NRL Memorandum Report 3178, Dec. 1975.

[9] Lofquist, K., "Internal waves produced by spheres moving in density stratified water", NBS Report 10267, 1970.

[10] Mei, C.C. and Wu, T.Y., "Gravity waves due to a point disturbance in a plane free surface flow of stratified fluids", Physics of Fluids, vol. 7, No. 8, 1964.

[11] Keller, J.B. and Munk, W.H., "Internal Wave Wakes of a Body Moving in a Stratified Fluid", The Physics of Fluids, vol. 13, No. 6, June 1970.

[12] Gilreath, H.E. and Brandt, A., "Experiments on the generation of internal waves in a stratified fluid", AIAA-83-1704, 1983.